A standardized index for assessing sub-monthly compound dry and hot conditions: application in China

Jun Li[1], Zhaoli Wang[1,2], Xushu Wu[1,2,*], Jakob Zscheischler[3,4], Shenglian Guo[5], Xiaohong Chen[6]

[1] *School of Civil Engineering and Transportation, State Key Laboratory of Subtropical Building Science, South China University of Technology, Guangzhou 510641, China.*

[2] *Guangdong Engineering Technology Research Center of Safety and Greenization for Water Conservancy Project, Guangzhou 510641, China.*

[3] *Climate and Environmental Physics, University of Bern, Sidlerstrasse 5, 3012 Bern, Switzerland.*

[4] *Oeschger Centre for Climate Change Research, University of Bern, Bern, Switzerland.*

[5] *State Key Laboratory of Water Resources and Hydropower Engineering Science, Wuhan University, Wuhan 430072, China.*

[6] *Center for Water Resource and Environment, Sun Yat-Sen University, Guangzhou 510275, China*

∗*Correspondence: xshwu@scut.edu.cn.*

Abstract: Compound dry-hot conditions pose large impacts on ecosystems and society worldwide. A suite of indices are proposed for the assessments of droughts and heatwaves previously, yet there is no index available for incorporating the joint variability of dry and hot conditions at sub-monthly scale. Here, we introduce a daily-scale index, termed as the standardized compound drought and heat index (SCDHI), to measure the intensity of compound dry and hot conditions. SCDHI is based on the daily drought index (the standardized antecedent precipitation evapotranspiration index (SAPEI)) and the standardized temperature index (STI) and a joint probability distribution method. The new index is verified against real-world compound dry and hot events and the related observed vegetation impacts in China. SCDHI can not only monitor the long-term compound dry and hot events, but also capture such events at sub-monthly scale and reflect the related vegetation activity impacts. The identified compound events generally persisted for 25-35 days and the southern China suffered from compound events most frequently. In future, the frequency, duration, severity and intensity of compound events increase throughout China in response to anthropogenic climate change, of which the frequency would generally increase by 1-3 times and the duration and severity increase by 50%; under largest emission scenario, duration, severity, and frequency across Midwest China increase by at least 3 times. The new index can provide a new tool to quantify sub-monthly characteristics of compound dry and hot events, conducive to the timely monitoring of their initiation, development, and decay which are vital for decision-makers and stake-holders to release early and timely warnings.

Keywords: compound event; SCDHI; SAPEI; sub-monthly scale; China

1 Introduction

Compound dry-hot event have been observed for all continents in recent decades (Hao et al., 2019; Mazdiyasni and AghaKouchak, 2015; Manning et al., 2019; Sutanto et al., 2020). The frequent compound dry-hot events have led to more devastating impacts on natural ecosystems and human society than individual events (Zscheischler et al., 2014, 2018; Chen et al., 2019; Hao et al., 2018a). Unfortunately, the extreme droughts and hots are expected to occur more frequently in the coming decades under global warming, which potentially results in more compound events in many parts of the world, especially for wet and humid regions (Wu et al., 2020; Swain et al., 2018, Zscheischler and Seneviratne, 2017a). Therefore, understanding such events are of crucial importance to provide the most fundamental information to help disaster mitigation.

Much effort has been made to study the compound events in recent years. Utilizing different thresholds to define the concurrent climate extremes for a specific period, the frequency of compound events has received a great deal of attention (Wu et al., 2019; Zhang et al., 2019). Although this approach can detect compound event occurrence, it fails to quantitatively measure compound event characteristics such as duration, severity, and intensity, and is inconvenient for comparison of compound event characteristics through different climates (Wu et al., 2020). Therefore, to overcome these shortages, several joint climate extreme indices have been proposed for analyzing the characteristics of the compound events. Specifically, the standardized dry and hot index based on the ratio of the marginal probability distribution functions of precipitation and temperature was proposed to measure the extreme degree of a compound drought and hot extreme event (Hao et al., 2018). Hao et al. (2019, 2020) recently proposed the standardized compound event indicator and compound dry-hot

index to assess the severity of compound dry and hot events by jointing the marginal distribution of standardized precipitation index (SPI) and standardized temperature index (STI) using the copula theory. These two joint indices provide useful tools to improve our understanding of the frequency, spatial extent and severity of the compound dry-hot event. However, they are inevitably subjected to some shortcomings including the fixed monthly scale and the disregard of evapotranspiration, which may limit their use in monitoring the detailed evolution of compound dry and hot events.

With the occurrence of extreme climate (e.g. high temperature, low humidity, and sunny skies), droughts can evolve rapidly (Koster et al., 2019; Otkin et al., 2018; Yuan et al., 2019; Li et al., 2020a). Such extreme weather can appear within a short period without resulting in long-lasting compound events, but rather, short-term droughts and heatwaves lasting a few weeks or even days (Mo and Lettenmaier, 2016; Zhang et al., 2019). Severe concurrent drought and heat can suddenly strike a region with a relatively short duration when extreme weather anomalies persist over the same region (Röthlisberger and Martius, 2019; Wang et al., 2016). Concurrent short-term drought and hot can pose greater potential socio-economic risks because the combination of these events can exacerbate their respective environmental and societal impacts (Kirono et al., 2017; Schumacher et al., 2019; Sedlmeier et al., 2018). Specifically, even short-term concurrent dry and hot extremes can lead to significant agricultural loss if they occur within sensitive stages in crop development such as emergence, pollination, and grain filling (Zhang et al., 2019). Under climate change, short-term concurrent dry and hot extremes are expected to increase (especially for humid regions), potentially causing substantial damage to natural ecosystems and society (Li et al., 2020b; Sun et al., 2019). To improve understanding of such short-term compound events and make early and timely warnings, decision-makers and stakeholders require more detailed

information such as the start time, severity, and the projected tendency in the coming days rather than the average state at a fixed monthly scale. Correspondingly, sub-monthly scale indices for characterizing short-term compound dry and hot events are needed. In addition, through the influence of evapotranspiration, short-term meteorological variables (e.g., temperature and radiation) are considered an important factor in drought and heatwave concurrences (James et al., 2010). Thus, the development of a compound drought and heat index should consider other important drought/hot-related factors including temperature and evapotranspiration.

The complexity of compound events makes it an unusual task to develop a simple and robust index to quantify their past and future changes (Zscheischler et al., 2020). A suite of indices are proposed for the assessments of droughts and heatwaves previously, yet there is no index available for incorporating the joint variability of dry and hot conditions at sub-monthly scale. Here we aim to formulate a compound drought and heat index, called the standardized compound drought and heat index (SCDHI), for monitoring and analyzing compound dry and hot events at sub-monthly scale. To achieve this aim, we combine a daily scale drought index, the standardized antecedent precipitation evapotranspiration index (SAPEI), which simultaneously considers precipitation and potential evapotranspiration, with a daily scale standardized temperature index (STI). We investigate the characteristics such as frequency, duration, severity, and intensity of compound dry-hot events during the historical (1961-2018) period and project their changes in China for the future (2050-2100) under different emission scenarios. This index can provide a new tool to quantify the characteristics of compound dry-hot event, and can monitor the compound dry-hot event at multiple time scale (e.g., daily, weekly and monthly) to provide detailed information on their initiation, development, decay, and trends.

2 Methods

2.1 data

Daily meteorological datasets covering 1961 to 2018 were collected from 2239 observational stations across the non-arid region in China (Fig. 1), which include precipitation, maximum air temperature, mean air temperature, minimum air temperature, relatively humidity, wind speed, and sunshine duration. All of these meteorological data with strict quality control are available from the China Meteorological Administration (http://cdc.nmic.cn/home.do) and the Resources and Environmental Science Data Center, Chinese Academy of Sciences (http://www.resdc.cn/Default.aspx). The observational station data were interpolated to 0.25× 0.25° gridded data by kriging method, as it yields higher interpolation accuracy than the other commonly used methods, e.g., ordinary nearest neighbor and inverse distance weighting (Liu et al., 2016). In this study, we only focus the non-arid region in China, because of three reasons: (1) replenishment of water resources across Chinese arid region is mainly from melted glacial or perennial frozen soil, but not from precipitation; (2) meteorological observations in Chinese arid regions are too scarce to conduct robust analysis (Wu et al., 2007; Xu et al., 2015); (3) from a practical perspective, calculating climate extreme indices across arid region with large-scale desert regions is less meaningless (Tomas-Burguera et al., 2020).

The two commonly used indices (i.e., monthly Palmer drought severity index (PDSI) and standardized precipitation evapotranspiration index (SPEI) were employed for comparison. PDSI and SPEI were computed from the same meteorological data described above. The conventional PDSI was empirically derived using the meteorological data of the central USA with its semi-arid climate. The portability of

the conventional PDSI is thus relatively poor (Liu et al., 2017). In this study, PDSI was calculated according to the China national standard of classification of meteorological drought with standard number of GB/T 20481-2017. The PDSI was built based on long-term meteorological data of in-situ stations evenly distributed around China, hence well monitor drought in China (Zhong et al., 2019a), and the detailed calculation on the PDSI is shown in supplementary materials. The 0.25°-daily root zone (0 - 100 cm) soil moisture dataset obtained from Community Land Model of the Global Land Data Assimilation System was also used in this study. Community Land Model product does not have explicit vertical levels, instead soil moisture is represented in surface (0-2cm), and root zone (0-100cm). Root zone soil moisture is chosen over the surface soil moisture on account of its appositeness to characterize drought, low noise relative to surface soil moisture (Hunt et al., 2009; Osman et al., 2020). The dataset from 1961 to 2014 were downloaded from the Goddard Earth Sciences Data and Information Services Center (Rodell et al., 2004). The soil moisture dataset from Community Land Model can well capture dry and wet conditions in China well (Bi et al., 2016; Feng et al., 2016). To avoid the effect of seasonality, the soil moisture was fitted by Gamma probability distribution, and then was standardized by normal quantile transformation. In addition, 8-day leaf area index of the MOD15A2H from 2003 to 2018 were collected. These data were resampled to 0.25° spatial resolution, and then the Z-score was used to calculate the leaf area index anomalies.

We further used eight global climate models from the Coupled Model Intercomparison Project Phase 5 (https://esgf.llnl.gov/) (Taylor et al., 2012), including CanESM2, CNRM-CM5, CSIRO-Mk3.6, MIROC-ESM, MPI-ESM-LR, BCC-CSM1-1, IPSL-CM5A-LR, and MRI-CGCM3, were used to project the future climate conditions. These global climate models exhibit good performance to simulate the key

features of precipitation and temperature in China (Jiang et al., 2016; Yang et al., 2019). We obtained daily climate variables (i.e., precipitation, temperature, relatively humidity, wind speed, and shortwave and longwave radiations) for the future (2050-2100) periods for the three Representative Concentration Pathways (RCPs) including RCP 2.6 (low emission scenario), RCP 4.5 (moderate emission scenario) and RCP 8.5 (high emission scenario). All of the global climate models' outputs were based on the first ensemble member of each model, referred to as *r1i1p1* in all of the experiments. In this study, the bias-corrected climate imprint method, one of the delta statistical downscaling methods, was used to downscale the global climate models outputs to a spatial resolution of 0.25° (Werner and Cannon, 2016). The detailed information on these global climate models is shown in Table S1.

2.2 Development of SCDHI

The SCDHI is a compound drought and heat index based on a daily drought index and the STI, which is computed in a similar fashion as the Standardized Precipitation Index (Zscheischler et al., 2014). The calculation of daily STI is similar to monthly STI, but for standardizing daily temperature. For example, with respect to one certain grid point, the 1 January STI are computed on the 1 January temperature datasets observed during 1961-2018 at each grid point. We firstly formulated a daily scale drought index, i.e. the SAPEI, by considering both precipitation and potential evapotranspiration. The Penman-Monteith method is used to calculate the potential evapotranspiration. Afterward, the joint distribution method was employed to compute the SCDHI.

2.2.1 Formulation of daily-scale drought index

Li et al. (2020b) have proposed the daily-scale drought index (SAPEI) that considers both precipitation and potential evapotranspiration. However, the primary limitation of this index is that it has a fixed temporal scale and cannot reflect the dry

and wet condition at different time scales. Hence, in this study, we developed the multiple time scale (i.e., 3-, 6-, 9-, and 12-month) daily drought index. Here, we followed the same nomenclature proposed by Li et al. (2020b) to refer to a daily standardized drought index (SAPEI) based on precipitation and potential evapotranspiration. SAPEI is simple to calculate, and uses the antecedent accumulative differences between precipitation and potential evapotranspiration to represent the dry and wet condition of the current day. The calculation procedure is described below.

The Penman-Monteith method (Allen et al., 1998) was firstly used to compute potential evapotranspiration. With a value for potential evapotranspiration, the daily difference between precipitation and potential evapotranspiration was calculated to reveal climatic water balance (precipitation minus potential evapotranspiration). To reflect dry and wet conditions of the day, the antecedent water surplus or deficit (WSD) was calculated through the following equations:

$$WSD = \sum_{i=1}^{n} \left(P - PET \right)_i \quad (1)$$

Where n is the number of previous days, PET represents the potential evapotranspiration, and P represents precipitation.

The WSD values can be aggregated at different time scales, such as 3, 6, 9 months, and so on. A probability distribution was used to fit the daily time series WSD. Given that different probability distributions may cause differences in drought indices (Stagge et al., 2015), to select the most suitable distribution, several commonly probability distributions including the general extreme value, log-logistic, lognormal, Pearson III, generalized Pareto, exponential, and normal distributions, should be used to fit the WSD series. In the study of Li et al. (2020b), Shapiro-Wilk and Kolmogorov-Smirnov test have been used applied for optimal probability distribution selection by comparing

the empirical probability distribution with a candidate theoretical probability distribution. They suggested that the log-logistic distribution is more suitable for SAPEI. Moreover, previous researches have demonstrated that the log-logistic distribution is suitable for standardizing drought indices, e.g. SPEI (Vicente-Serrano et al., 2010). Therefore, we chose the log-logistic distribution to compute SAPEI. Once the daily WSD series were fit to a probability distribution, cumulative probabilities of the WSD series were obtained and transformed to standardized units (SAPEI) using the classical approach of Barton et al. (1965).

2.2.2 Construction of SCDHI

The SCDHI was established through copula theory (a brief introduction on copula theory is shown in supplementary materials), which can combine the candidate variables into one numerical expression. This approach not only realizes a projection from multiple dimensions to a single dimension, but also the marginal distributions of the candidate variables combined with their original structures can be fully preserved within the constructed joint distribution. Hence, the copula-based index provides an objective description of the compound events (Hao et al., 2018b; Terzi et al., 2019).

There are many copula families available, which have widely been used for jointing bivariate distributions (Terzi et al., 2019). Among then, Clayton, Gumbel, Normal, T, and Frank copula perform well for jointing bivariate hydrometeorological variables (Ayantobo et al., 2018; Liu et al., 2019), and thus were employed to establish the bivariate joint probability distribution in this study. Assuming, the two random Gaussian variables X and Y representing SAPEI and STI, respectively, the compound dry-hot event can be identified as one variable X lower than or equal to a threshold x, and the other variable Y higher than a threshold y at the same time. The joint

probability p of the compound dry-hot event can then be expressed as:

$$p = P(X \le x, Y \ge y) = u - c(u,v) \quad (2)$$

where u was the X marginal distribution, and $c(u,v)$ was the joint probability distribution.

This joint cumulative probability p could be treated as an indicator, where smaller p values denote more severe condition of compound dry-hot event. However, p to the given marginal sets, p values in different seasons or areas reflected different conditions and are thus not comparable. Hence, the joint probability p was transformed to a uniform distribution by fitting a distribution F, which was then standardized as an indicator to characterize compound dry-hot events. Once the p series at each day were fitted to a copula, the p series were transformed to standardized units. SCDHI can be estimated by taking the inverse of joint cumulative probability (p) as:

$$SCDHI = \varphi^{-1}(F(P(X \le x, Y \ge y))) \quad (3)$$

where φ is the standard normal distribution function. the distribution F was estimated based on the Yeo-Johnson transformation formula (Yeo and Johnson, 2000).

Following the categories of compound dry and hot conditions as suggested by (Wu et al., 2020), we defined five categories of compound dry and hot conditions, including abnormal, light, moderate, heavy and extreme compound drought-hot, as shown in Table 1.

We used Akaike information criterion, Bayesian information Criterion, and Kolmogorov-Smirnov statistics as goodness-of-fit measures to select an appropriate copula. These statistical measures have been commonly used for estimating the goodness of fit of a proposed cumulative distribution function to a given empirical distribution function (Liu et al., 2019; Terzi et al., 2019). The statistics of the three metrics are presented in Fig. S1-3. According to the evaluation metrics, the Frank copula was utilized to establish the joint probability function and construct SCDHI in this study. Note that the SCDHI under three future scenarios is also used the Frank copula, while the parameters are assessed by future scenarios data. The SCDHI development was illustrated in Fig. S4.

Furthermore, to verify the ability of SCDHI to capture the compound dry and hot event, three verification metrics were used (i.e., probability of detection, false alarm ratio, and critical success index) (Winston and Ruthi, 1986).

$$Probability\ of\ detection = hit/(hit + miss) \tag{4}$$

$$False\ alarm\ ratio = false\ alarm/(hit + false\ alarm) \tag{5}$$

$$Critical\ success\ index = hit/(hit + false\ alarm + miss) \tag{6}$$

where *hit* (observed drought-hot) refers to the number of grids when SAPEI and STI is subjected to grade 1-4 and SCDHI is subjected to grade 1-4; *Miss* denotes the number of grids when SAPEI and STI is between grade 1-4 and SCDHI is subjected to other grades than grade 1-4; *False alarm* denotes the number of grids when SAPEI and STI is subjected to other grades than grade 1-4 but SCDHI is subjected to grades of grade 1-4.

3 Results and Discussion

3.1 Evaluation of SAPEI

The SCDHI was established based on the STI and daily-scale drought index, i.e., SAPEI. However, no previous studies have tested the (daily) drought monitoring performance of SAPEI. When developing a drought index, rigorous testing is required with respect to its applicability before it is applied in drought monitoring. Fig. 2 shows the spatial distributions and density of the correlations between SAPEI and SPEI/PDSI/soil moisture across China. The monthly mean SAPEI at 3-, 6-, 9- and 12-month scale all showed strong agreement with the SPEI in China, with correlation coefficients higher than 0.8 ($p < 0.01$), indicating that the monthly SAPEI at multiple time scale calculated from the daily value could have the same capability of monthly drought monitoring as SPEI. The 3-, 6-, 9- and 12-month SAPEI generally showed good correlation with PDSI, and 3-month SAPEI and PDSI generally correlate closely, with correlation coefficients higher than 0.6 ($p < 0.01$). For daily SAPEI at 12-month scale and soil moisture, a close correlation was detected in south and north China, while relatively weak correlation is found in Midwest China. The correlation between SAPEI and soil moisture increased in magnitude at time scales of 3-9 months. For 12-month SAPEI, mean correlation coefficient reached about 0.5 for whole China. This phenomenon implied that the short-time scale SAPEI was more sensitive to precipitation change, and thus could be more suitable for meteorological drought, while the long-time scale (more than five month) SAPEI was more closely related to soil moisture and can be applied for agricultural drought monitoring. Overall, these analyses indicate that the SAPEI at daily and monthly scale showed reliability in drought monitoring.

To further test the drought monitoring performance of the SAPEI, typical drought

events were chosen as case studies. During recent decades, several well-known large-scale drought events have hit China, including the droughts in winter of 2009 to spring of 2010, and in 2011 (Lu et al., 2014; Yu et al., 2019). In this study, the drought regimes during these events were taken as case studies to evaluate the drought monitoring performance of SAPEI at 3-month time scales (Sun and Yang, 2012). We firstly showed the monthly evolution of these events by the monthly mean SAPEI, SPEI, and PDSI, and then analyzed the daily evolution of drought in space and time in the most affected areas according to SAPEI and soil moisture.

3.2.1 Drought events during 2009-2010

As shown in Fig. S5, the monthly evolution in 2009/10 drought based on SAPEI was generally similar with that of SPEI and PDSI. This drought started to appear in most of China (except for the central and northeast China) in September 2009, and then persisted in most of China during October to December 2009. During January and April in 2010, severe drought persisted in southwest China, while drought in the rest of China gradually disappeared in this period. After that, dry conditions in southwest China gradually relieved from May to June in 2010, but did not disappear.

Despite being located in the humid climate zone, southwest China suffered from exceptional drought during the autumn of 2009 to the spring of 2010 (Lin et al., 2015). During this drought, more than 16 million people and 11 million livestock faced drinking water shortages, with direct economic losses estimated at 19 billion yuan in southwest China (Lin et al., 2015). We selected this event in southwest China as the first case study, and reveal detailed spatial and temporal change of this event at daily scale based on SAPEI and soil moisture (Fig. 3 and 4). During September 1 to 30 of 2009, the drought started to appear in the region, and dry conditions became worse and spread throughout nearly the entire southwest China from October 1 to November 15

of 2009. Severe dry conditions then stayed in the region for 152 days from November 15 to April 15 of 2010, with high intensity. Afterwards, severe drought was gradually relieved from April 15 to June 15. The drought diminished over time in most parts of southwest China by the end of June.

3.2.2 Drought events in 2011

As shown in Fig. S6. The 2011 drought monthly pattern monitored by SAPEI are generally consistent with those by SPEI and PDSI. The drought mainly started in north China in January, while in March it spread to most of China, and severe dry conditions persisted in most areas during April to May. In August, the drought mainly moved to southward. Severe drought persisted in southwest China during September and October, but it then gradually faded away. The results monitored by the SAPEI are generally consisted with the findings of Lu et al. (2014).

The 2011 drought event was particularly unusual in the middle and lower reaches of the Yangtze River Basin (MLR-YRB). The MLR-YRB is generally in a wet condition, nevertheless, suffered its worst drought in the 50 years during the spring. The severe drought caused shortage of drinking water for 4.2 million people. 3.7 million hectares of crops were damaged or destroyed. Moreover, the heavy drought led to more than 1,300 lakes devoid of all water in Hubei province (Xu et al., 2015). The temporal and spatial evolution of this event in MLR-YRB described by daily SAPEI and soil moisture was shown in Fig. 5-6. The drought started to appear in the north part of the MLR-YRB in early February of 2011, and then gradually expanded to the whole MLR-YRB during early February and March 15. The severe drought condition persisted in this region for 78 days (from March 15 to May 31). Afterwards, there was a tendency toward alleviating drought conditions, and most of MLR-YRB was under light and moderate drought conditions.

The previous detailed analysis showed that the SAPEI not only captures monthly characteristics of droughts, but also has the potential to track droughts at sub-monthly scale (Li et al., 2020b). Though the input data (including precipitation and potential evapotranspiration) of SAPEI are similar to SPEI, the rationale of the index is different from SPEI. It was calculated for each day and considers the water surplus or deficit of that day and the previous days. SPEI was commonly employed to monitor and analyze the monthly or longer-scale droughts (Vicente-Serrano et al., 2010). It thus may not be appropriate to apply the SPEI at shorter timescales (e.g., daily or weekly), because of the inherent problem in the construction of the index. Although SPEI gives a full and equal consideration to the water surplus or deficit in the period of the considered time scale, it does not consider the water surplus or deficit in the days before the period. If the scale is very short, this may cause problems. For a 7-day period, for example, if there is no precipitation during the period, it may be regarded as a drought period when compared with historical records (the method used by the SPEI); however, if there is a heavy precipitation just before the period, then the 7-day period probably remains wet and is unlikely to experience drought condition during such a short time. Previous studies have demonstrated the disadvantage of SPEI for short-time scale drought monitoring (Lu, 2009; Lu et al., 2014; Li et al., 2020b).

Soil moisture would be the most appropriate variable for agriculture drought monitoring and analyses (Mishra and Singh, 2010). However, there are few long-term and large-scale observational soil moisture datasets due to insufficient observation stations around the world, especially for developing regions, which limits it wide use in drought monitoring and analyses (Seneviratne et al., 2010). Thus, using observational hydrometeorological datasets, the complex physical process models, such as the variable infiltration capacity model, are widely used to simulate the soil moisture

(Liang et al., 1996; Xia et al., 2018). However, running such models requires highly trained personnel not usually available at local agencies. In addition, when the model is used locally, it generally needs to be calibrated and verified by observational datasets (Xia et al., 2018; Zhou et al., 2019). This certainly limits the wide use of soil moisture as a drought indicator.

In summary, the SAPEI meets the requirements of a drought index, given the fact that it shows reliable and robust ability for drought analysis and monitoring. Like the SPEI, SAPEI includes multiple time scales (3-, 6-, 9-, and 12- month) to monitor droughts at monthly resolution and is relatively sensitive to soil moisture variation. However, SAPEI has the advantage over SPEI regarding sub-monthly drought monitoring. Such an index could help fill a gap between science and applications in that it would be operationally tractable for detecting and monitoring both short-term and sustained droughts.

3.2 Evaluation of SCDHI

The SCDHI was developed by joining the marginal distribution of the SAPEI and STI. Though the copula method has been widely utilized to connect bivariate distribution, the property of SCDHI in capturing compound dry-hot events still needs to be tested. Fig. 7 shows the spatial pattern and density for probability of detection, false alarm ratio, and critical success index when the drought and hot events observed by SAPEI and STI, respectively, were related to compound drought-hot event detected by SCDHI at 3-, 6-, 9- and 12-monthly scale. As shown in Fig. 7, probability of detection is close to 1 and false alarm ratio is close to 0, implying that SCDHI can well detect in most of the areas where the droughts and hots were detected by SAPEI and STI. The values of critical success index indicated that the ratios of drought-hot affected areas detected by SAPEI and STI to the drought and hot areas detected by SCDHI were

close to one. Overall, these analyses implied that SCDHI can well monitor droughts and hots that can be successfully captured by SAPEI and STI. The SCDHI thus detects compound dry-hot events that are identified separately by the coincidence of low SAPEI and high STI. In addition, the SCDHI detects events that are very extreme in either the SAPEI or the STI and moderate in the other variable but thus still cause substantial damage (Zscheischler et al., 2017b). Furthermore, the SCDHI is able to quantify the magnitude of compound dry-hot events.

To further test the drought-heat monitoring performance of the SCDHI, two typical compound dry-hot events were chosen as case studies according to the Yearbook of Meteorological Disasters in China. One was a well-known compound drought and heatwave striking Sichuan-Chongqing region with serious consequences during summer of 2006 (Wu et al., 2020), and the other occurred in southern China with adverse impacts on agriculture during July to September of 2009 (Wang et al., 2010). Sichuan-Chongqing region experienced continuous extreme temperature during mid-June to late August 2006. The duration and severity of this hot event were the worst on the historical record. Simultaneously, a heavy drought occurring once in 100 years hit this region. During this compound event, a population of over ten million was confronted with drinking water shortage, about twenty thousand km^2 of cropland suffered serious losses, and more than one hundred times forest fire broke out. Local governments issued the most serious arid warning (Zhang et al., 2008). Thus, we take this typical drought-hot event as first case studies to evaluate the drought/hot monitoring performance of SCDHI. The monthly spatial pattern of this compound event in Sichuan-Chongqing region is shown in Fig. S7, indicating that Sichuan-Chongqing region during summer in 2006 experienced the moderate to extreme compound dry and hot conditions. Fig. 8 maps the spatial pattern of this compound event and its impact on

vegetation from mid-June to late August. This event started to appear in Sichuan-Chongqing region in mid-June 2006, and gradually spread throughout the whole Sichuan-Chongqing region during June 19 to 26. The moderate dry-hot condition then persisted in the entire Sichuan-Chongqing region from June 27 to August 5 in 2006, lasting for 40 days. The negative leaf area index was scattered in some of the dry-hot affected areas. However, during August 6 to 21, the drought-hot event became even more severe with the onset of extremely hot temperatures, causing negative vegetation anomalies in most of the affected areas.

The monthly spatial pattern of another compound event in southern China during July to September of 2009 is shown in Fig. S8. Overall moderate to heavy compound dry and hot conditions are observed at monthly scale in this region. However, this event showed large fluctuation at weekly scale. According to the Yearbook, the hot event was divided into two periods: the first stage was from early to late July, and the other stage was from mid-August to early September. The fluctuating compound event caused adverse impact of crop pollination and grain filling, resulting in decrease of crop production. Fig. 9 maps the spatial pattern of this event and its impact on leaf area index. In the first stage, the drought-hot event hit the most of southern China during July 5 to 12, and then it became severe in the west part of southern China during July 13 to 20. However, the hot event suddenly disappeared from July 21 to 28, leading to disappearance of the compound event in most of southern China (Fig. 9a). Afterward, the compound event hit this region again from August 6 to 13, and its intensity was strong during August 14 to 21, with severe hot conditions. Subsequently, the intensity and spatial extent of the compound event faded away in north of southern China during August 22 to 29. This event extended to most of this region again from August 30 to September 14, with severe dry and hot condition. The compound events still stayed in

this region from September 15 to 22 (Fig. 9b). Despite the short-term event, the anormal change in vegetation was found in most of the dry-hot affected areas. This complex event indicates that monthly analyses of the event can provide an overall situation, but is not be able to capture the serious dry and hot conditions caused by a short-term extreme climate anomaly at shorter time scales. Though such short-term compound event only lasted for days or weeks, they lead to large agricultural losses if they occur within sensitive stages in crop development (i.e., pollination and grain filling) (Mazdiyasni and AghaKouchak, 2015). To provide timely information of the compound dry-hot events, short-time scale analyses and monitoring of such events are essential.

Overall, the changes in these two compound dry-hot events based on SCDHI are consistent with the national weather records (http://www.weather.com.cn/zt/kpzt/) and the Yearbook of Meteorological Disasters in China 2010. In summary, the SCDHI is able to robustly and reliably capture compound dry-hot events at sub-monthly scale, and potentially provide a new tool to objectively and quantitatively analyze and monitor the characteristics of compound dry-hot events in time and space.

3.3 Application

Here, we evaluate and compare the spatiotemporal variation of characteristics of compound dry-hot events in China during growing season (April-September), because such events can more easily cause adverse impact on agriculture and ecosystem during these periods (Hao et al., 2018; Wu et al., 2019). More precisely, the compound dry-hot events from 1961 to 2018 were identified based on 3-month scale SCDHI and run theory (Wu et al., 2018), after which the frequency, duration, severity, and intensity of these events were analyzed (A specific case to identify compound dry-hot event is shown in Fig. S9). We then projected their future characteristics changes under the RCP

2.6, 4.5 and 8.5 from 2050 to 2100. Given that short-term concurrent dry and hot events generally persist for at least weeks (Otkin et al., 2018), only the events lasting for more than two weeks were considered in this study.

Fig. 10 shows spatial patterns of characteristics of the compound dry-hot events. A high frequency of compound events was detected in southern China, with occurrence of every two years on average, in contrast, the eastern Tibet Plateau and northeast China experienced fewer compound events (Fig. 10a), which was generally consistent with the previous studies (Liu et al., 2020; Wang et al., 2016). The compound dry-hot event generally lasted for about twenty-five to thirty-five days in most of China, while in east Tibet Plateau, the compound dry-hot event persisted for less than twenty days (Fig. 10b). The severity and intensity of the compound dry-hot event presented relatively similar patterns and showed that most of eastern China experienced high severity and intensity (Fig. 10c-d). Overall, southern China suffered more frequent compound dry-hot events, with higher severity and intensity. Southern China is a humid region where evapotranspiration is mainly controlled by energy supply because soil moisture is usually sufficient. For given adequate soil moisture in the initiation of drought, evaporative demand can increase rapidly during a short period when strong, transient meteorological changes (such as extreme temperature) occur, which in turn exhaust soil moisture to intensify drought conditions (Zhang et al., 2019, Otkin et al., 2018). Moreover, vegetation over south China is usually abundant and plants tend to suck more water from the soil when high temperatures occur, causing evapotranspiration increase and soil moisture decline (Li et al., 2020c; Wang et al., 2016). More surface sensible heat fluxes are thus transferred to the near-surface atmosphere to further increase air temperatures (Mo and Lettenmaier, 2015). These land-atmosphere interactions altogether cause the Bowen ratio to increase (Otkin et al., 2013, 2018), creating a

favorable condition for short-term concurrence droughts and hots. Therefore, compound dry-hot event is more likely to occur in humid regions with higher severity and intensity.

Fig. 11 illustrates the spatial patterns of change in frequency, duration, severity, and intensity of the compound dry-hot events under RCP 2.6, 4.5, and 8.5 scenarios. According to Fig. 11a, the future (2050-2100) compound dry-hot event frequency under three scenarios in most of east China will increase by about one to three times with respect to the reference period (1961-2018). Under RCP 8.5 scenario, compound dry-hot event at about 4% of the study region is expected to markedly increase by more than five times, which are scattered in the central to west parts of China. The duration of compound dry-hot event across the east of the study region will mainly show an increase of about 0.5 times, while duration in mid-west China potentially increases by approximately 1.5 times under RCP 8.5 scenarios (Fig. 11b). The spatial pattern of future severity change is similar to the duration; severity in most of east China is projected to increase by about 0.5 time under three scenarios; however, compound dry-hot event severity over mid-west China is expected to more than triple under RCP 8.5 (Fig. 11c). The compound dry-hot event intensity in most of the study region exhibits slight increase for all scenarios in comparison to the historical period.

Global warming is very likely to exacerbate the prevalence of the compound dry-hot events (Pfleiderer et al., 2019). The cumulative density functions of the future variations in compound dry-hot event characteristics considering only temperature and all variable changes were quantified, and the result is shown in Fig. 12. The frequency and intensity of the future variations in compound dry-hot event do not show large difference between two scenarios, while duration and severity display great increase due to temperature variation, as marked by the movement towards the right side of the

cumulative density curves. Increasing temperature could lead to remarkable increase evapotranspiration, and thus causing more surface sensible heat fluxes into atmosphere (Mo and Lettenmaier, 2015; Zhang et al., 2019). These land-atmosphere interactions altogether cause the Bowen ratio to increase (Otkin et al., 2013, 2018), creating a favorable condition for concurrence dries and hots. In short, temperature could be generally the primary factor increasing the compound dry-hot severity and duration (Cook et al., 2014). In addition, trends are often present in individual variables, while can also occur in the dependence between drivers of compound events, which consequently affects associated risks. The (negative) correlation between seasonal mean summer temperature and precipitation is projected to intensify in many land regions, leading to more frequent extremely dry and hot conditions (Kirono et al., 2017; Zscheischler and Seneviratne, 2017a), while variation in compound dry-hot event due to the complex interaction between climate variables is need further studied (Zscheischler et al., 2020). Overall, the frequency, severity, duration, and intensity of the compound dry-hot events in China under global warming will increase significantly. Effective measures need to be implemented to decrease the CO^2emissions for compound dry and hot event mitigation.

4 Conclusions

Under global warming, the compound dry and hot event tends to more frequent and short-lived (i.e., days or weeks). Correspondingly, a compound drought and heat index should be able to monitor such event at sub-monthly scales in order to timely reflect dry and hot condition evolution. In this study, we developed a multiple time scale (e.g., 3-, 6-, 9, and 12- month) compound drought and heat index, termed as SCDHI, to monitor short-time (e.g., days or weeks) and long-time (e.g., months) compound event. This index was established based on the daily drought index (i.e., SAPEI) and

Standardized Temperature Index (STI) using a joint probability distribution method. Using the SCDHI, we then quantitively investigated the characteristics (i.e., frequency, intensity, severity, and duration) of the compound dry-hot events in China in historical period (1961-2018), and revealed how they would change in the future (2050-2100) under representative concentration pathway (RCP) 2.6, 4.5, and 8.5 scenarios. The main conclusions of this study are presented as follows: The SCDHI can well monitor simultaneous dries and hots detected by SAPEI and STI. The monthly SCDHI can provide an overall situation of the compound dry and hot conditions, but sub-monthly SCDHI can well capture fluctuation of simultaneous dries and hots within a month. It also can reflect the impact of the compound dry and hot event on vegetation anomalies. The SCDHI can offer a new tool to quantitatively measure the characteristics of the compound dry-hot events. It also can provide detailed information such as the initiation, development, decay, and tendency of the compound event for decision-makers and stakeholders to make early and timely warning. In the case study of the China, the southern China suffered more frequent the compound dry-hot event, with higher severity and intensity. The compound dry-hot event mainly lasted for twenty-five to thirty-five days in China. The frequency, duration, severity, and intensity of compound events will intensify throughout the China in future. The frequency will increase by about one to three times with respect to the reference period. A region with fewer compound event (< 5) would exhibit a multi-fold (more than five times) increase in the future. The duration across east areas mainly increased by 0.5 times, while severity project to increase by about 0.5 to 1 times.

Data availability. The observed meteorological datasets are available at http://cdc.nmic.cn/home.do. The CMIP5 datasets are available at https://esgf.llnl.gov.

Author Contributions. Conceived and designed the experiments: JL, SW. Performed the experiments: JL, SW. Analyzed the data: JL. Wrote and edited the paper: JL, SW, ZW, JZ, SG, XC.

Competing interests. The authors declare that they have no conflict of interest.

Acknowledgement

The research is financially supported by the National Natural Science Foundation of China (51879107, 51709117), the Guangdong Basic and Applied Basic Research Foundation (2019A1515111144), and the Water Resource Science and Technology Innovation Program of Guangdong Province (2020-29).

References

Allen, R. G., Pereira, L. S., Raes, D. and Smith, M.: Crop evapotranspiration: Guidelines for computing crop requirements, Irrig. Drain. Pap. No. 56, FAO, doi:10.1016/j.eja.2010.12.001, 1998.

Ayantobo, O. O., Li, Y., Song, S., Javed, T. and Yao, N.: Probabilistic modelling of drought events in China via 2-dimensional joint copula, J. Hydrol., 559, 373–391, doi:10.1016/j.jhydrol.2018.02.022, 2018.

Barton, D. E., Abramovitz, M. and Stegun, I. A.: Handbook of Mathematical Functions with Formulas, Graphs and Mathematical Tables., J. R. Stat. Soc. Ser. A,

doi:10.2307/2343473, 1965.

Bi, H., Ma, J., Zheng, W. and Zeng, J.: Comparison of soil moisture in GLDAS model simulations and in situ observations over the Tibetan Plateau, J. Geophys. Res., doi:10.1002/2015JD024131, 2016.

Chen, L., Chen, X., Cheng, L., Zhou, P. and Liu, Z.: Compound hot droughts over China: Identification, risk patterns and variations, Atmos. Res., 227(May), 210–219, doi:10.1016/j.atmosres.2019.05.009, 2019.

Cook, B. I., Smerdon, J. E., Seager, R., and Coats, S.: Global warming and 21 st century drying. Climate Dynamics, 43(9-10), 2607-2627, 2014.

Feng, X., Fu, B., Piao, S., Wang, S., Ciais, P., Zeng, Z., Lü, Y., Zeng, Y., Li, Y., Jiang, X. and Wu, B.: Revegetation in China's Loess Plateau is approaching sustainable water resource limits, Nat. Clim. Chang., doi:10.1038/nclimate3092, 2016.

Ford, T. W., McRoberts, D. B., Quiring, S. M. and Hall, R. E.: On the utility of in situ soil moisture observations for flash drought early warning in Oklahoma, USA, Geophys. Res. Lett., doi:10.1002/2015GL066600, 2015.

Hao, Z., Hao, F., Singh, V. P., Xia, Y., Shi, C. and Zhang, X.: A multivariate approach for statistical assessments of compound extremes, J. Hydrol., 565, 87–94, doi:10.1016/j.jhydrol.2018.08.025, 2018a.

Hao, Z., Hao, F., Singh, V. P. and Zhang, X.: Quantifying the relationship between compound dry and hot events and El Niño–southern Oscillation (ENSO) at the global scale, J. Hydrol., 567, 332–338, doi:10.1016/j.jhydrol.2018.10.022, 2018b.

Hao, Z., Hao, F., Singh, V. P. and Zhang, X.: Statistical prediction of the severity of compound dry-hot events based on El Niño-Southern Oscillation, J. Hydrol., 572, 243–250, doi:10.1016/j.jhydrol.2019.03.001, 2019.

Hunt, E. D., Hubbard, K. G., Wilhite, D. A., Arkebauer, T. J. and Dutcher, A. L.: The

development and evaluation of a soil moisture index. Int. J. Climatol., 29(5), 747-759, doi.org/10.1002/joc.1749, 2009.

James, S., Complex, B., Black, S. J., Health, O. and Ando, H.: The synergy between drought and extremely hot summers in the Mediterranean, Biochem. J., 2010.

Jiang, D., Tian, Z. and Lang, X.: Reliability of climate models for China through the IPCC Third to Fifth Assessment Reports, Int. J. Climatol., doi:10.1002/joc.4406, 2016.

Kirono, D. G. C., Hennessy, K. J. and Grose, M. R.: Increasing risk of months with low rainfall and high temperature in southeast Australia for the past 150 years, Clim. Risk Manag., doi:10.1016/j.crm.2017.04.001, 2017.

Koster, R. D., Schubert, S. D., Wang, H., Mahanama, S. P. and Deangelis, A. M.: Flash drought as captured by reanalysis data: Disentangling the contributions of precipitation deficit and excess evapotranspiration, J. Hydrometeorol., doi:10.1175/JHM-D-18-0242.1, 2019.

Liang, X., Wood, E. F., and Lettenmaier, D. P.: Surface soil moisture parameterization of the VIC-2L model: Evaluation and modification. Global and Planetary Change, 13(1-4), 195-206, 1996.

Li, J., Wang, Z., Wu, X., Chen, J., Guo, S., and Zhang, Z.: A new framework for tracking flash drought events in space and time. Catena, 194, 104763, 2020a.

Li, J., Wang, Z., Wu, X., Xu, C.-Y., Guo, S. and Chen, X.: Toward Monitoring Short-Term Droughts Using a Novel Daily-Scale, Standardized Antecedent Precipitation Evapotranspiration Index, J. Hydrometeorol., 891–908, doi:10.1175/jhm-d-19-0298.1, 2020b.

Li, J., Wang, Z., Wu, X., Guo, S., and Chen, X.: Flash droughts in the Pearl River Basin, China: Observed characteristics and future changes. Sci. Total Environ., 707,

136074, 2020c.

Lin, W., Wen, C., Wen, Z. and Gang, H.: Drought in Southwest China: A Review, Atmos. Ocean. Sci. Lett., 8(6), 339–344, doi:10.3878/AOSL20150043, 2015.

Liu, Z., Wang, Y., Shao, M., Jia, X., Li, X: Spatiotemporal analysis of multiscalar drought characteristics across the Loess Plateau of China. J. Hydrol., 534, 281-299, doi.org/10.1016/j.jhydrol.2016.01.003, 2016,

Liu, Y., Zhu, Y., Ren, L., Singh, V. P., Yang, X. and Yuan, F.: A multiscalar Palmer drought severity index, Geophys. Res. Lett., 44(13), 6850–6858, doi:10.1002/2017GL073871, 2017.

Liu, Y., Zhu, Y., Ren, L., Yong, B., Singh, V. P., Yuan, F., Jiang, S. and Yang, X.: On the mechanisms of two composite methods for construction of multivariate drought indices, Sci. Total Environ., 647, 981–991, doi:10.1016/j.scitotenv.2018.07.273, 2019.

Liu, Y., Zhu, Y., Zhang, L., Ren, L., Yuan, F., Yang, X. and Jiang, S.: Flash droughts characterization over China: From a perspective of the rapid intensification rate, Sci. Total Environ., doi:10.1016/j.scitotenv.2019.135373, 2020.

Lu, E.: Determining the start, duration, and strength of flood and drought with daily precipitation: Rationale, Geophys. Res. Lett., 36(12), 1–5, doi:10.1029/2009GL038817, 2009.

Lu, E., Cai, W., Jiang, Z., Zhang, Q., Zhang, C., Higgins, R. W. and Halpert, M. S.: The day-to-day monitoring of the 2011 severe drought in China, Clim. Dyn., 43(1–2), 1–9, doi:10.1007/s00382-013-1987-2, 2014.

Mo, K. C. and Lettenmaier, D. P.: Heat wave flash droughts in decline, Geophys. Res. Lett., doi:10.1002/2015GL064018, 2015.

Mo, K. C. and Lettenmaier, D. P.: Precipitation deficit flash droughts over the United

States, J. Hydrometeorol., doi:10.1175/JHM-D-15-0158.1, 2016.

Mazdiyasni, O. and AghaKouchak, A.: Substantial increase in concurrent droughts and heatwaves in the United States, Proc. Natl. Acad. Sci. U. S. A., 112(37), 11484–11489, doi:10.1073/pnas.1422945112, 2015.

Manning, C., Widmann, M., Bevacqua, E., Van Loon, A. F., Maraun, D. and Vrac, M: Increased probability of compound long-duration dry and hot events in Europe during summer (1950-2013). Environmental Research Letters, 14(9), 094006, 2019.

Osman, M., Zaitchik, B. F., Badr, H. S., Christian, J. I., Tadesse, T., Otkin, J. A. and Anderson, M. C.: Flash drought onset over the Contiguous United States: Sensitivity of inventories and trends to quantitative definitions, Hydrol. Earth Syst. Sci. Discuss., doi.org/10.5194/hess-2020-385, in review, 2020.

Otkin, J. A., Anderson, M. C., Hain, C., Mladenova, I. E., Basara, J. B. and Svoboda, M.: Examining rapid onset drought development using the thermal infrared-based evaporative stress index, J. Hydrometeorol., doi:10.1175/JHM-D-12-0144.1, 2013.

Otkin, J. A., Svoboda, M., Hunt, E. D., Ford, T. W., Anderson, M. C., Hain, C. and Basara, J. B.: Flash droughts: A review and assessment of the challenges imposed by rapid-onset droughts in the United States, Bull. Am. Meteorol. Soc., 99(5), 911–919, doi:10.1175/BAMS-D-17-0149.1, 2018.

Pfleiderer, P., Schleussner, C. F., Kornhuber, K. and Coumou, D.: Summer weather becomes more persistent in a 2 °C world, Nat. Clim. Chang., 9(9), 666–671, doi:10.1038/s41558-019-0555-0, 2019.

Rodell, M., Houser, P. R., Jambor, U., Gottschalck, J., Mitchell, K., Meng, C. J., Arsenault, K., Cosgrove, B., Radakovich, J., Bosilovich, M., Entin, J. K., Walker, J. P., Lohmann, D. and Toll, D.: The Global Land Data Assimilation System, Bull.

Am. Meteorol. Soc., doi:10.1175/BAMS-85-3-381, 2004.

Röthlisberger, M. and Martius, O.: Quantifying the Local Effect of Northern Hemisphere Atmospheric Blocks on the Persistence of Summer Hot and Dry Spells, Geophys. Res. Lett., doi:10.1029/2019GL083745, 2019.

Schumacher, D. L., Keune, J., van Heerwaarden, C. C., Vilà-Guerau de Arellano, J., Teuling, A. J. and Miralles, D. G.: Amplification of mega-heatwaves through heat torrents fuelled by upwind drought, Nat. Geosci., 12(9), 712–717, doi:10.1038/s41561-019-0431-6, 2019.

Sedlmeier, K., Feldmann, H. and Schädler, G.: Compound summer temperature and precipitation extremes over central Europe, Theor. Appl. Climatol., doi:10.1007/s00704-017-2061-5, 2018.

Stagge, J. H., Tallaksen, L. M., Gudmundsson, L., Van Loon, A. F. and Stahl, K.: Candidate Distributions for Climatological Drought Indices (SPI and SPEI), Int. J. Climatol., doi:10.1002/joc.4267, 2015.

Seneviratne, S. I., Corti, T., Davin, E. L., Hirschi, M., Jaeger, E. B., Lehner, I., .and Teuling, A. J.: Investigating soil moisture–climate interactions in a changing climate: A review. Earth-Science Reviews, 99(3-4), 125-161, 2010.

Sun, C. and Yang, S.: Persistent severe drought in southern China during winter-spring 2011: Large-scale circulation patterns and possible impacting factors, J. Geophys. Res. Atmos., doi:10.1029/2012JD017500, 2012.

Sun, C. X., Huang, G. H., Fan, Y., Zhou, X., Lu, C. and Wang, X. Q.: Drought Occurring With Hot Extremes: Changes Under Future Climate Change on Loess Plateau, China, Earth's Futur., 7(6), 587–604, doi:10.1029/2018EF001103, 2019.

Swain, D. L., Langenbrunner, B., Neelin, J. D. and Hall, A.: Increasing precipitation volatility in twenty-first-century California, Nat. Clim. Chang., 8(5), 427–433,

725 doi:10.1038/s41558-018-0140-y, 2018.
726 Taylor, K. E., Stouffer, R. J. and Meehl, G. A.: An overview of CMIP5 and the
727 experiment design, Bull. Am. Meteorol. Soc., doi:10.1175/BAMS-D-11-00094.1,
728 2012.
729 Terzi, S., Torresan, S., Schneiderbauer, S., Critto, A., Zebisch, M. and Marcomini, A.:
730 Multi-risk assessment in mountain regions: A review of modelling approaches for
731 climate change adaptation, J. Environ. Manage., 232(September 2018), 759–771,
732 doi:10.1016/j.jenvman.2018.11.100, 2019.
733 Vicente-Serrano, S. M., Beguería, S. and López-Moreno, J. I.: A multiscalar drought
734 index sensitive to global warming: The standardized precipitation
735 evapotranspiration index, J. Clim., 23(7), 1696–1718,
736 doi:10.1175/2009JCLI2909.1, 2010.
737 Wang, L., Yuan, X., Xie, Z., Wu, P. and Li, Y.: Increasing flash droughts over China
738 during the recent global warming hiatus, Sci. Rep., doi:10.1038/srep30571, 2016.
739 Wang, W., Wang, W. J., Li, J. S., Wu, H., Xu, C. and Liu, T.: The impact of sustained
740 drought on vegetation ecosystem in southwest China based on remote sensing, in
741 Procedia Environmental Sciences., 2010.
742 Werner, A. T. and Cannon, A. J.: Hydrologic extremes - An intercomparison of multiple
743 gridded statistical downscaling methods, Hydrol. Earth Syst. Sci.,
744 doi:10.5194/hess-20-1483-2016, 2016.
745 Winston, H.A., Ruthi, L.J.: Evaluation of RADAP II severe-storm-detection algorithms.
746 Bull. Am. Meteorol. Soc., 67(2), 145-150, doi.org/10.1175/1520-
747 0477(1986)067<0145:EORISS>2.0.CO;2 1986.
748 Wu, J., Chen, X., Yao, H., Liu, Z. and Zhang, D.: Hydrological Drought Instantaneous
749 Propagation Speed Based on the Variable Motion Relationship of Speed-Time

Process, Water Resour. Res., doi:10.1029/2018WR023120, 2018.

Wu, X., Hao, Z., Hao, F. and Zhang, X.: Variations of compound precipitation and temperature extremes in China during 1961–2014, Sci. Total Environ., 663, 731–737, doi:10.1016/j.scitotenv.2019.01.366, 2019.

Wu, X., Hao, Z., Zhang, X., Li, C. and Hao, F.: Evaluation of severity changes of compound dry and hot events in China based on a multivariate multi-index approach, J. Hydrol., 583, 124580, doi:10.1016/j.jhydrol.2020.124580, 2020.

Xia, Y., Mocko, D. M., Wang, S., Pan, M., Kumar, S. V., and Peters-Lidard, C. D.: Comprehensive evaluation of the variable infiltration capacity (VIC) model in the North American Land Data Assimilation System. Journal of Hydrometeorology, 19(11), 1853-1879, 2018.

Xu, C., McDowell, N. G., Fisher, R. A., Wei, L., Sevanto, S., Christoffersen, B. O., Weng, E. and Middleton, R. S.: Increasing impacts of extreme droughts on vegetation productivity under climate change, Nat. Clim. Chang., 9(12), 948–953, doi:10.1038/s41558-019-0630-6, 2019.

Xu, K., Yang, D., Yang, H., Li, Z., Qin, Y. and Shen, Y.: Spatio-temporal variation of drought in China during 1961-2012: A climatic perspective, J. Hydrol., doi:10.1016/j.jhydrol.2014.09.047, 2015.

Yang, Y., Bai, L., Wang, B., Wu, J. and Fu, S.: Reliability of the global climate models during 1961–1999 in arid and semiarid regions of China, Sci. Total Environ., doi:10.1016/j.scitotenv.2019.02.188, 2019.

Yeo, I. N. K. and Johnson, R. A.: A new family of power transformations to improve normality or symmetry, Biometrika, 87(4), 954–959, doi:10.1093/biomet/87.4.954, 2000.

Yu, H., Zhang, Q., Xu, C. Y., Du, J., Sun, P. and Hu, P.: Modified Palmer Drought

775 Severity Index: Model improvement and application, Environ. Int., 130(January),
776 104951, doi:10.1016/j.envint.2019.104951, 2019.
777 Yuan, X., Wang, L., Wu, P., Ji, P., Sheffield, J. and Zhang, M.: Anthropogenic shift
778 towards higher risk of flash drought over China, Nat. Commun.,
779 doi:10.1038/s41467-019-12692-7, 2019.
780 Zhang, W. J., Lu, Q. F., Gao, Z. Q. and Peng, J.: Response of remotely sensed
781 normalized difference water deviation index to the 2006 drought of eastern
782 Sichuan Basin, Sci. China, Ser. D Earth Sci., 51(5), 748–758, doi:10.1007/s11430-
783 008-0037-0, 2008.
784 Zhang, Y., You, Q., Chen, C. and Li, X.: Flash droughts in a typical humid and
785 subtropical basin: A case study in the Gan River Basin, China, J. Hydrol., 551,
786 162–176, doi:10.1016/j.jhydrol.2017.05.044, 2017.
787 Zhang, Y., You, Q., Mao, G., Chen, C. and Ye, Z.: Short-term concurrent drought and
788 heatwave frequency with 1.5 and 2.0 °C global warming in humid subtropical
789 basins: a case study in the Gan River Basin, China, Clim. Dyn., 52(7–8), 4621–
790 4641, doi:10.1007/s00382-018-4398-6, 2019.
791 Zhong, R., Chen, X., Lai, C., Wang, Z., Lian, Y., Yu, H. and Wu, X.: Drought
792 monitoring utility of satellite-based precipitation products across mainland China,
793 J. Hydrol., 568(June 2018), 343–359, doi: 10.1016/j.jhydrol.2018.10.072, 2019a.
794 Zhong, R., Zhao, T., He, Y. and Chen, X.: Hydropower change of the water tower of
795 Asia in 21st century: A case of the Lancang River hydropower base, upper
796 Mekong, Energy, 179, 685–696, doi:10.1016/j.energy.2019.05.059, 2019b.
797 Zscheischler, J., Michalak, A. M., Schwalm, C., Mahecha, M. D. and Zeng, N.: Impact
798 of large-scale climate extremes on biospheric carbon fluxes: An intercomparison
799 based on MsTMIP data, Global Biogeochem. Cycles, 28(6), 585–600,

doi:10.1002/2014GB004826, 2014.

Zscheischler, J., Orth, R. and Seneviratne, S. I.: Bivariate return periods of temperature and precipitation explain a large fraction of European crop yields, Biogeosciences, doi:10.5194/bg-14-3309-2017, 2017a.

Zscheischler, J. and Seneviratne, S. I.: Dependence of drivers affects risks associated with compound events, Sci. Adv., 3(6), 1–11, doi:10.1126/sciadv.1700263, 2017b.

Zscheischler, J., Westra, S., Van Den Hurk, B. J. J. M., Seneviratne, S. I., Ward, P. J., Pitman, A., Aghakouchak, A., Bresch, D. N., Leonard, M., Wahl, T. and Zhang, X.: Future climate risk from compound events, Nat. Clim. Chang., 8(6), 469–477, doi:10.1038/s41558-018-0156-3, 2018.

Zscheischler, J., Martius, O., Westra, S., Bevacqua, E. and Raymond, C.: A typology of compound weather and climate events, Nat. Rev. Earth Environ., doi: https://doi.org/10.1038/s43017-020-0060-z, 2020.

Zhou, J., Wu, Z., He, H., Wang, F., Xu, Z., and Wu, X.: Regional assimilation of in situ observed soil moisture into the VIC model considering spatial variability. Hydrological Sciences Journal, 64(16), 1982-1996, 2019.

Table

Table 1 Categories of compound dry and hot conditions based on SCDHI.

Category	Dry-hot condition	SCDHI
Grade 0	Abnormal	(-0.80, -0.50]
Grade 1	Light	(-1.30, -0.80]
Grade 2	Moderate	(-1.60, -1.30]
Grade 3	Heavy	(-2.0, -1.60]
Grade 4	Extreme	≤ -2

Figure

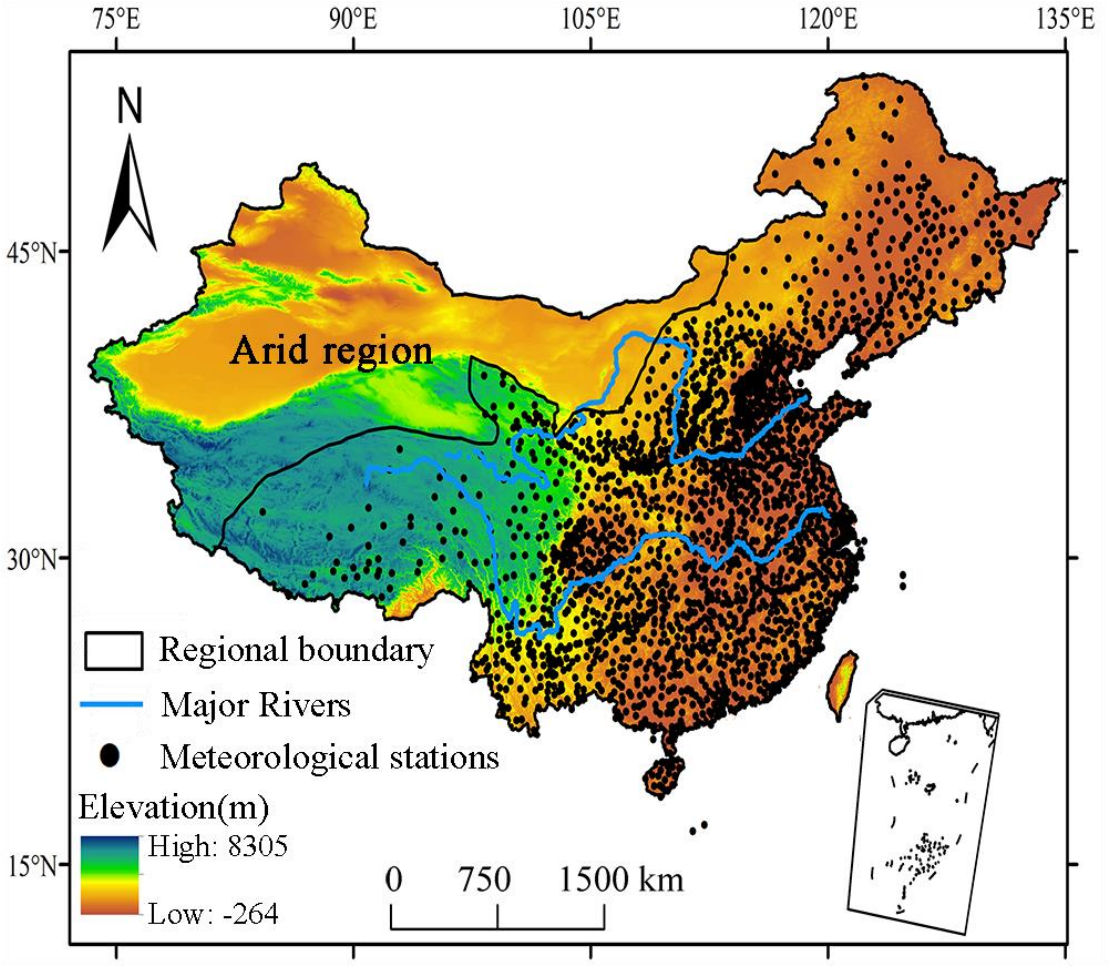

Figure 1 Geographical position of China and local of meteorological stations.

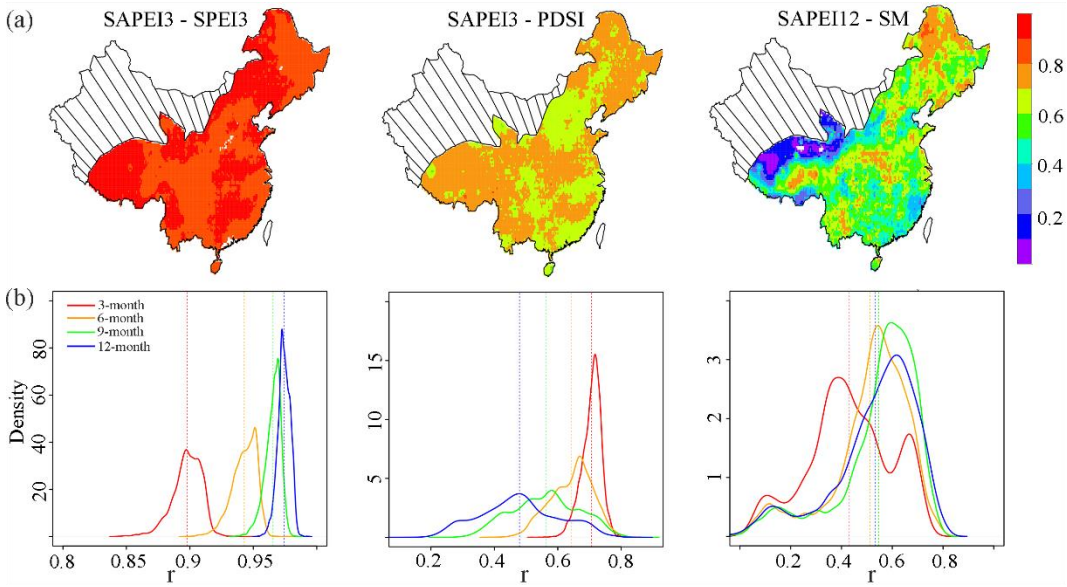

Figure 2 (a) The spatial pattern of the correlations between monthly SAPEI and SPEI/PDSI, and between daily SAPEI and soil moisture (SM), and (b) The density plot for the correlation coefficients between SAPEI and SPEI/PDSI/SM. The monthly SAPEI is computed by averaging the daily values in each month.

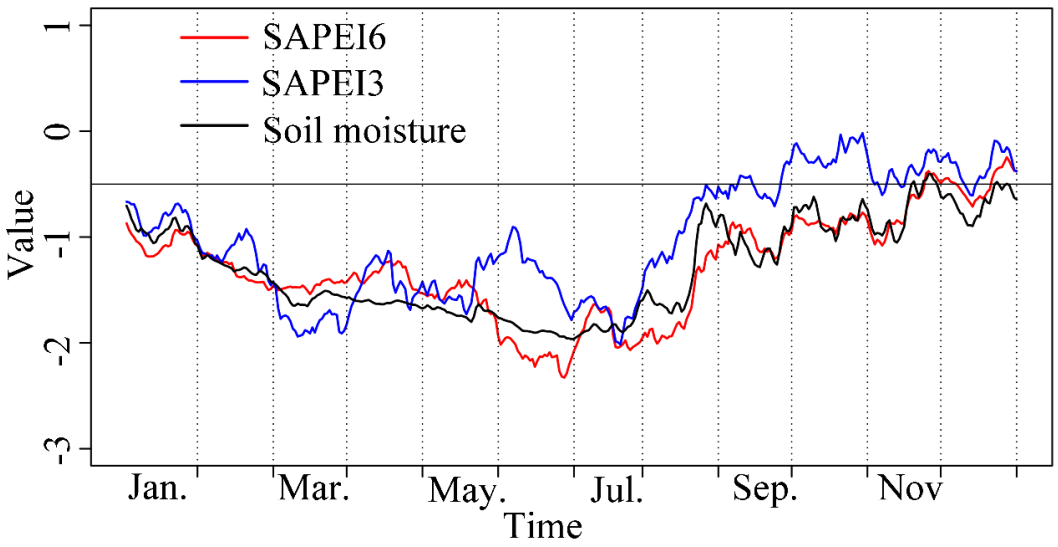

Figure 3 SAPEI and soil moisture series during the 2009/2010 drought event over the southwest China. The series were spatially average merged series. The value of solid black line is at -0.5, indicating the distinction between drought and non-drought.

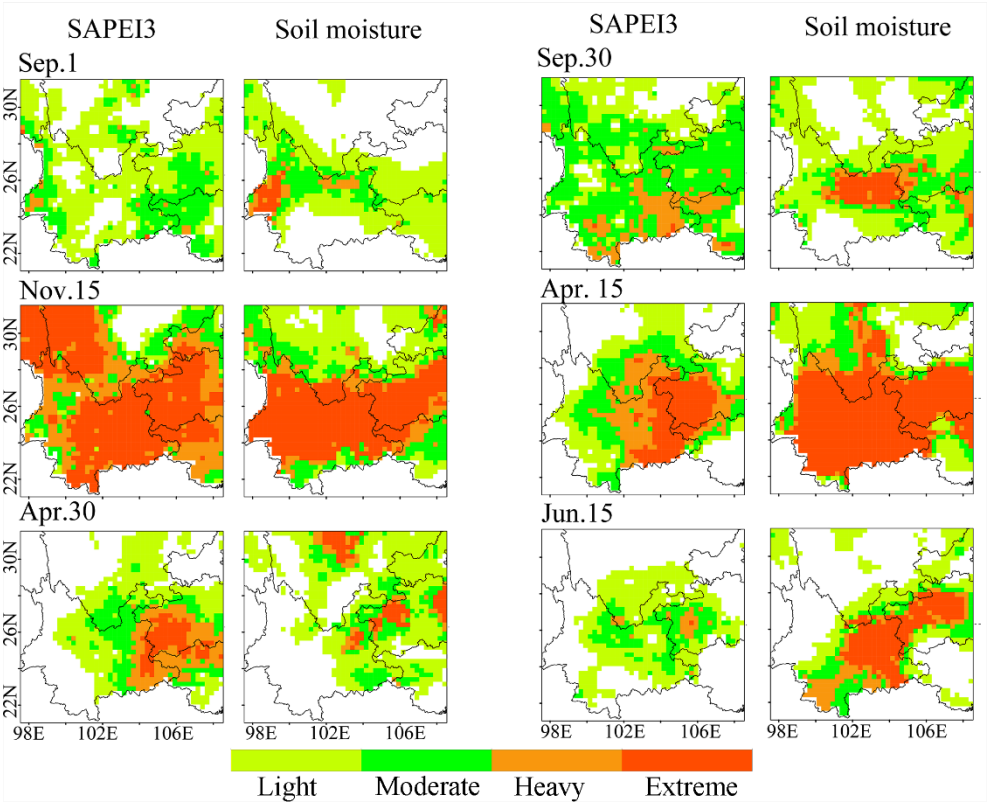

871

872 Figure 4 Daily evolutions of the 2009/2010 drought event over the southwest China

873 monitored by 3-month SAPEI and soil moisture.

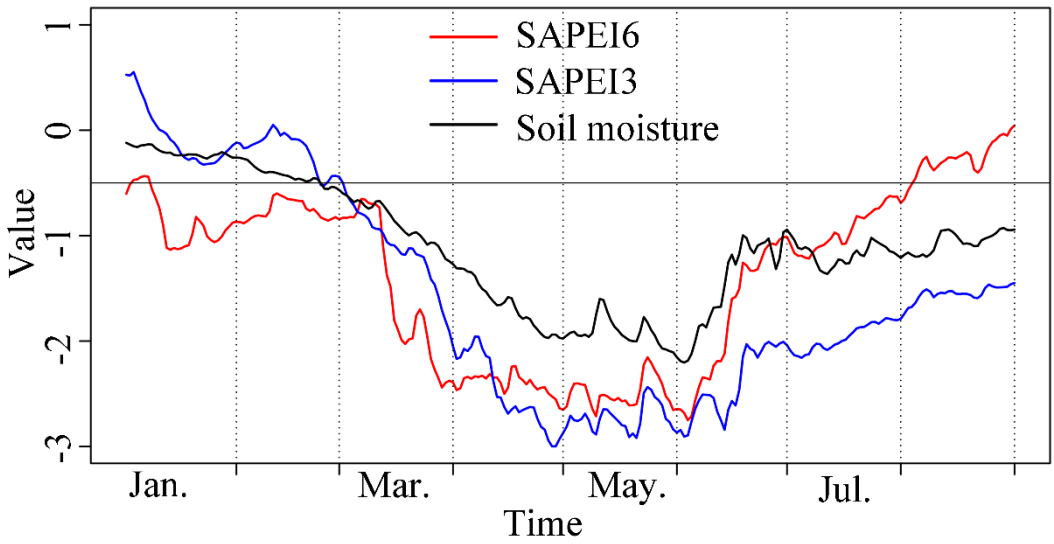

874

875 Figure 5 SAPEI (3- and 6-month) and soil moisture series during the 2011 drought

876 event over the middle and lower reaches of the Yangtze River. The series were spatially

877 average merged series. The value of solid black line is at -0.5, indicating the distinction

878 between drought and non-drought.

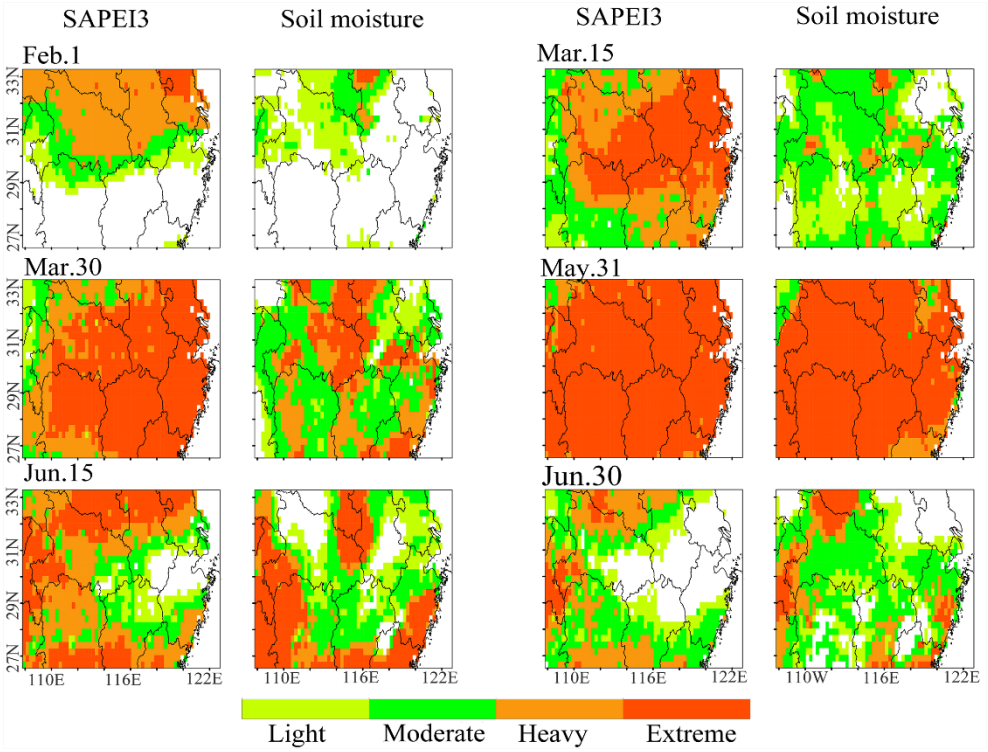

Figure 6 Daily evolutions of the 2011 drought event over the middle and lower reaches of the Yangtze River monitored by 3-month SAPEI and soil moisture.

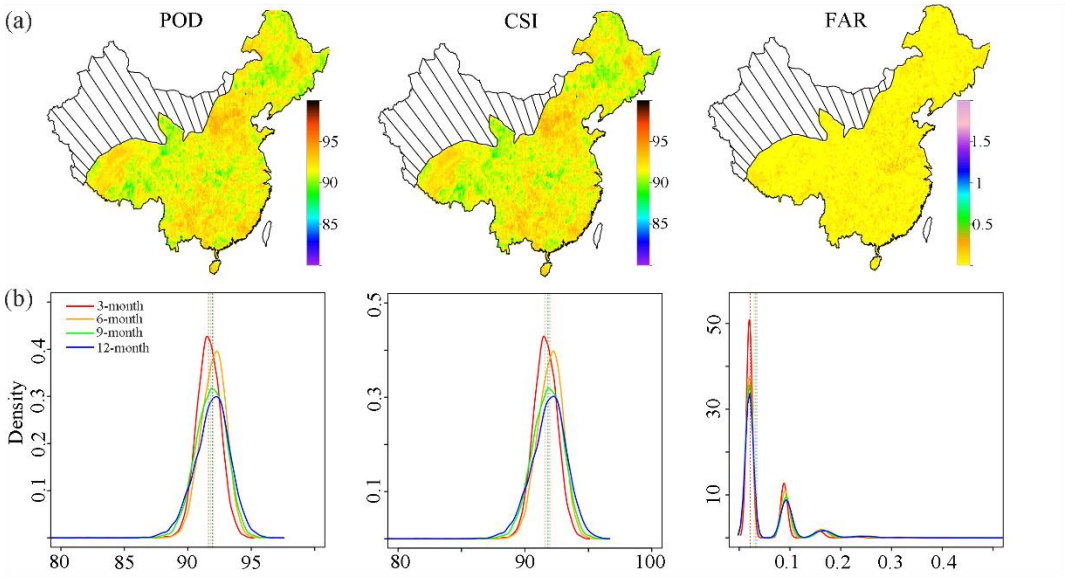

Figure 7 (a) The spatial pattern of probability of detection (POD, %), critical success index (CSI, %), and false alarm ratio (FAR, %) for 3-month SCDHI from 1961 to 2018, and (b) Density plot for POD, FAR, and CSI for 3-, 6-, 9-, 12-month SCDHI from 1961 to 2018.

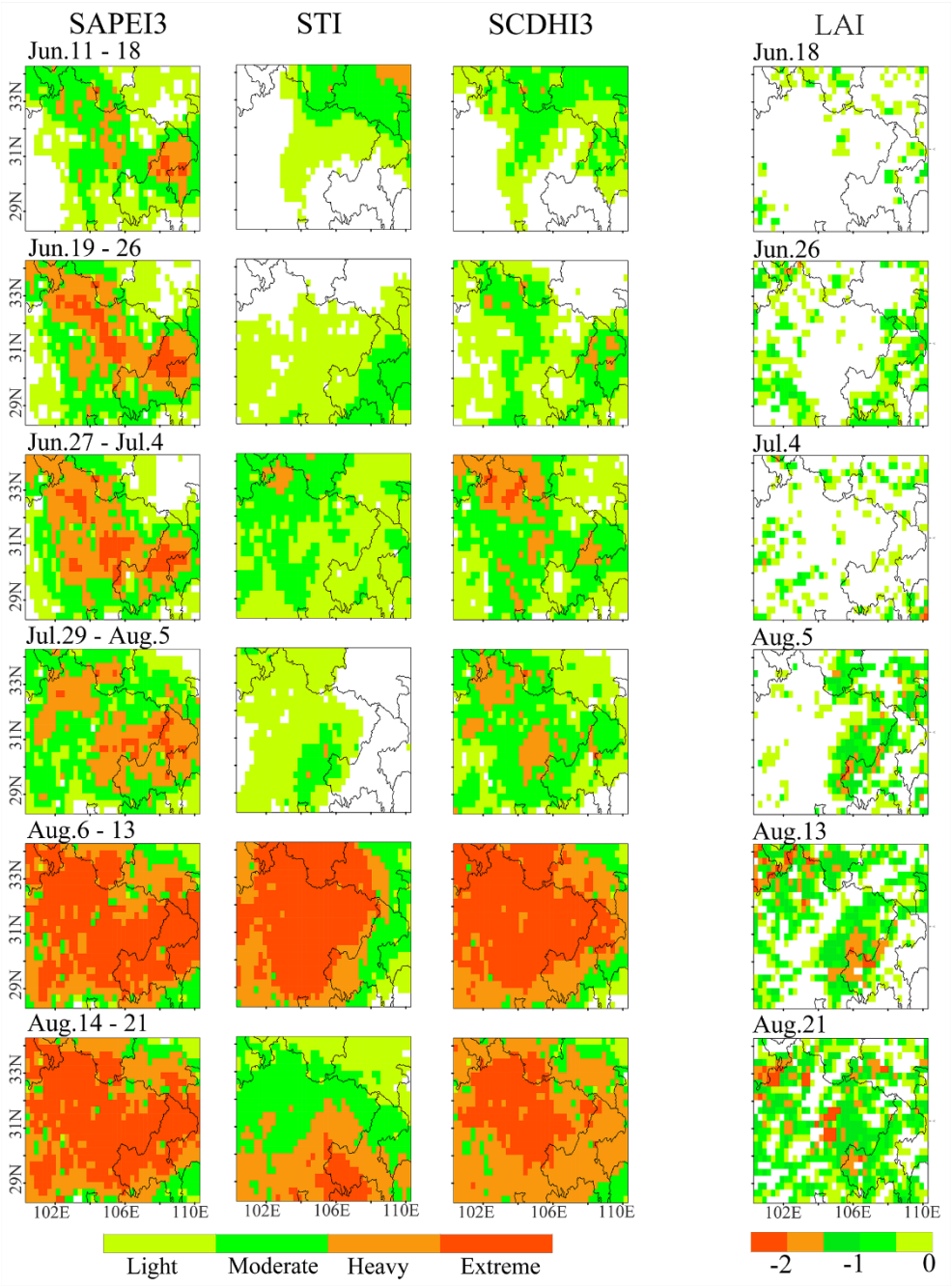

888

889 Figure 8 The spatial evolutions of the compound dry and hot event over the Sichuan-

890 Chongqing region in 2006 and its impact on vegetation.

891

892

893

894

895

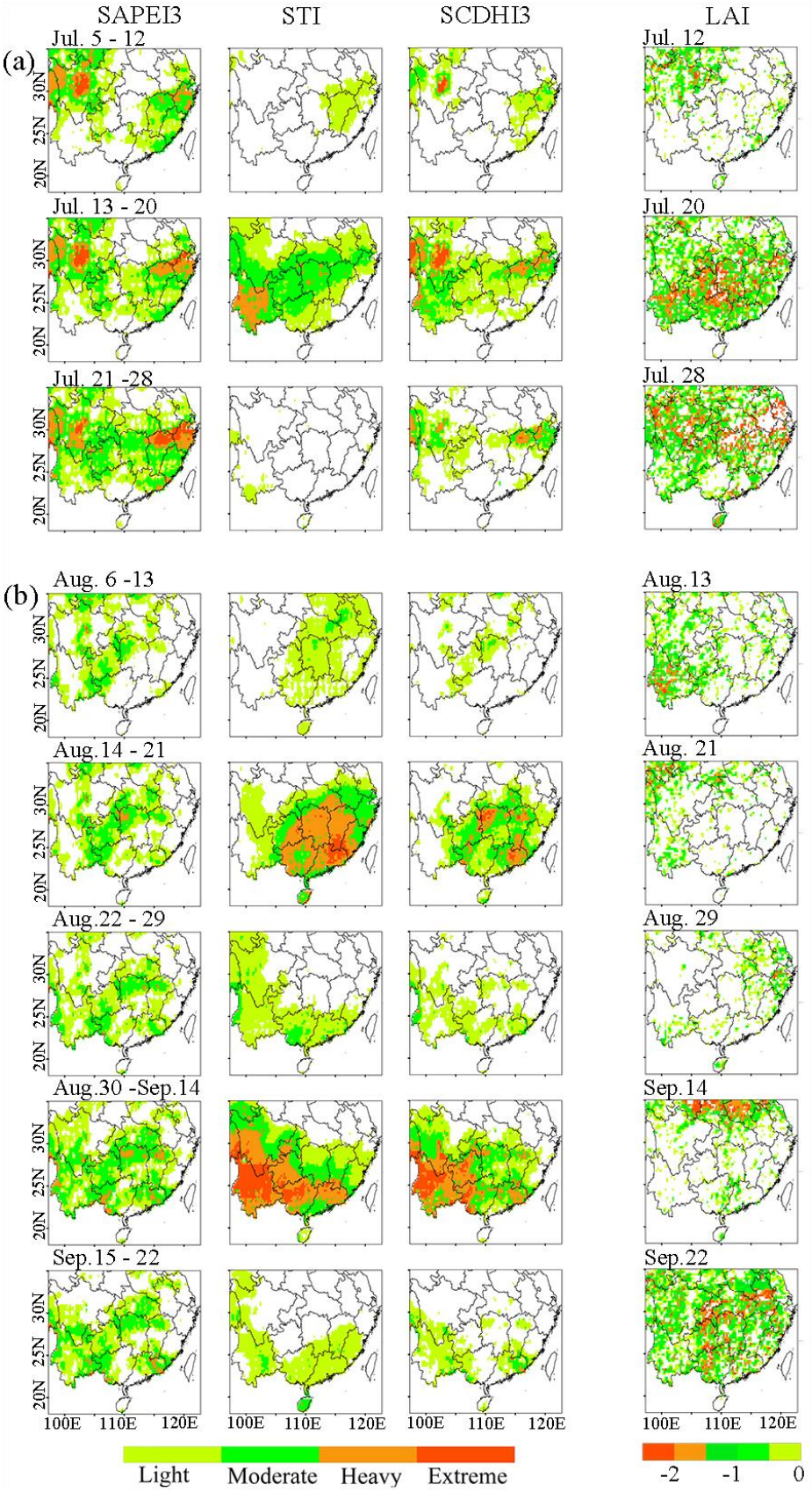

Figure 9 The spatial evolutions of the compound dry and hot event over the southern China in 2009 and its impact on vegetation.

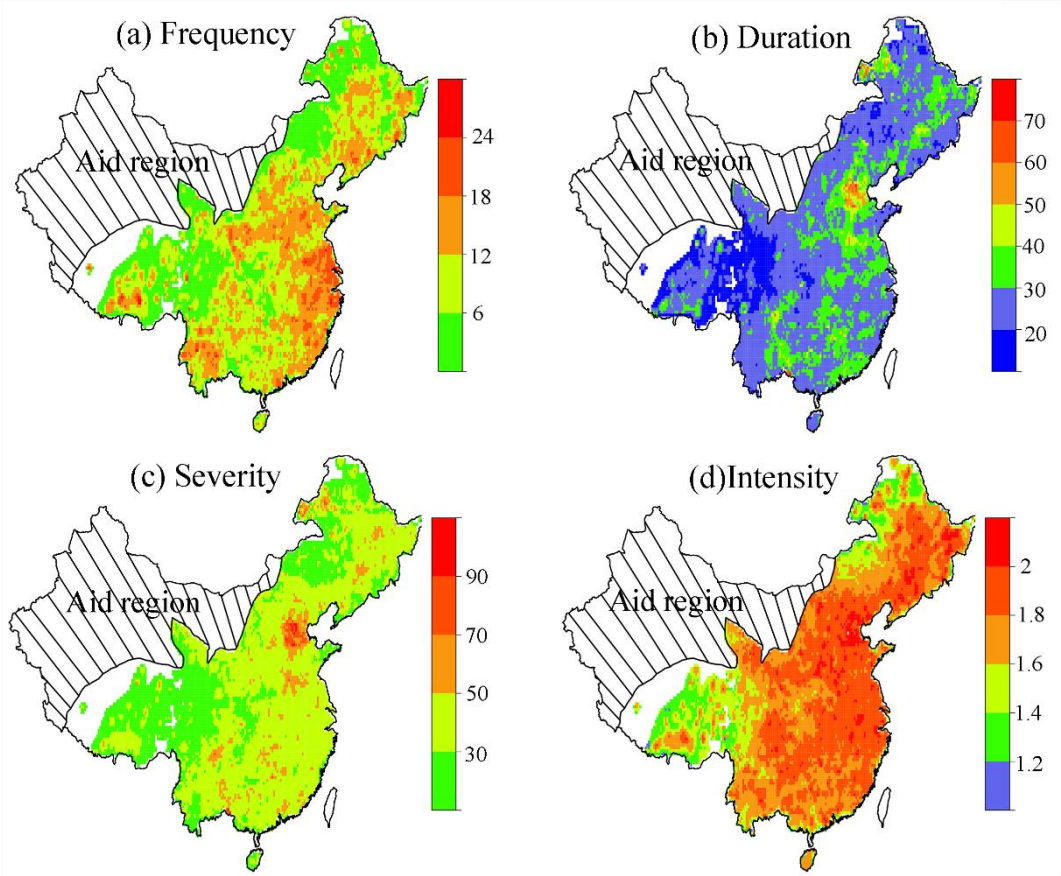

Figure 10 The spatial pattern of the characteristics of the compound dry and hot event in China from 1961 to 2018.

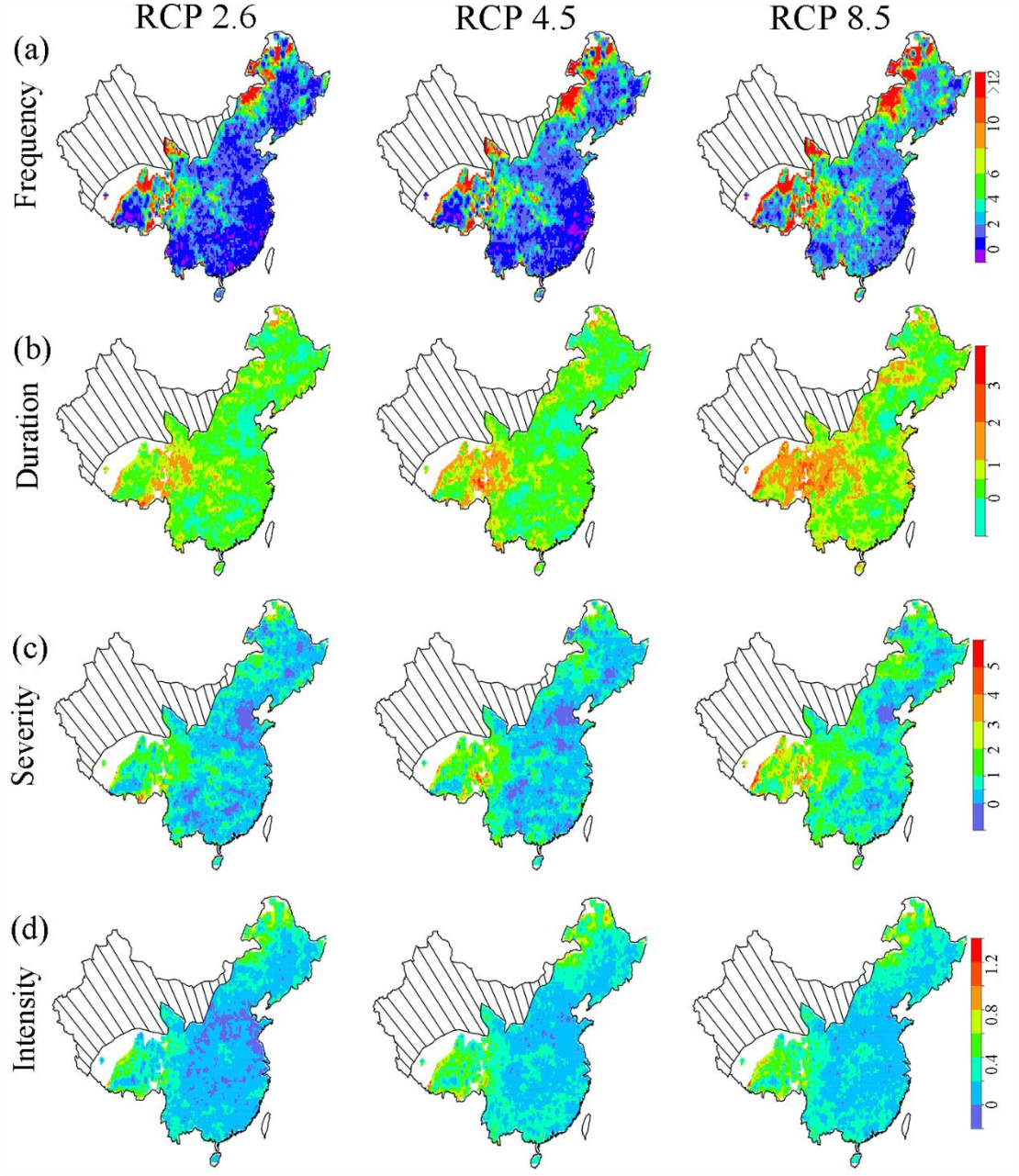

911

912 Figure 11 Future changes in characteristics of the compound dry and hot events under
913 the RCP 2.6, RCP4.5 and RCP8.5 scenarios. The change values were the ratio of the
914 future value to the reference values. Reference period: 1961-2018, and future period:
915 2050-2100.

916

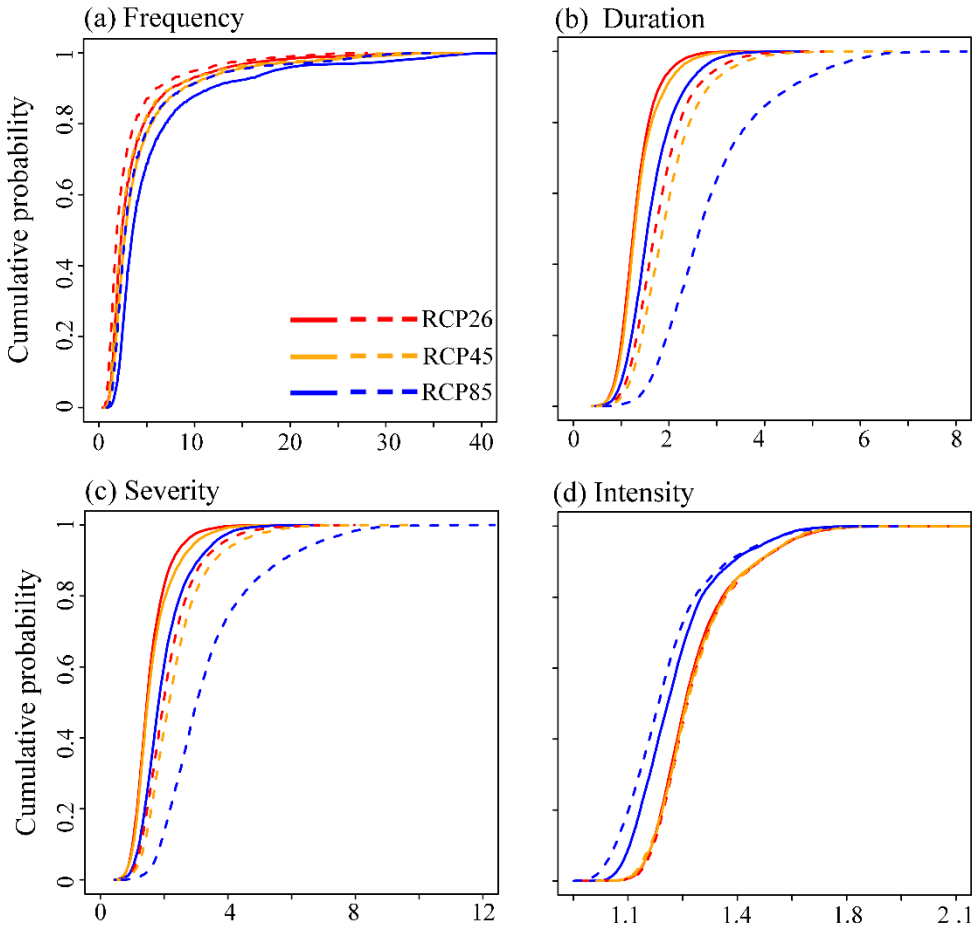

Figure 12 Cumulative probability of future changes (multiple) in of the compound dry-hot event characteristics. The dash lines indicate future characteristics changes only considered temperature change, while solid lines represent the future changes driven by all variable variation.